Chapter 2

ZnO Nanorods/PCDTBT: PCBM: PbS QDs Based High Performance Inverted Structure Broadband Photodetectors

Content of this Chapter

Part of this work has been published as:

- **Deep Chandra Upadhyay et al.,** "High-Performance Inverted Structure Broadband Photodetector Based on ZnO Nanorods/PCDTBT:PCBM:PbS QDs," in ***IEEE Transactions on Electron Devices***, vol. 67, no. 11, pp. 4970-4976, Nov. 2020, doi: 10.1109/TED.2020.3026984. (IF: **2.913**)

Chapter 2

ZnO Nanorods/PCDTBT: PCBM: PbS QDs Based High Performance Inverted Structure Broadband Photodetectors

2.1 Introduction

We have already discussed in Chapter-1 that the broadband photodetectors with a detection spectrum ranging from ultraviolet to near-infrared (NIR) find potential applications in biomedicine, imaging, communication, environmental monitoring and defense [1]–[8].]. Organic semiconductors have been extensively explored for developing broad band photodetectors due to their low-cost, easy solution-processed fabrication methodology and flexible nature [9]–[13]. Researchers have made several attempts for enhancing the spectral response of the organic photodetectors by incorporating semiconducting nanoparticles (NPs) and quantum dots (QDs) as sensitizer [28-29], [79-80] or inserting low band gap organic semiconducting materials into the active region [[12], [17]].

In recent times, a significant progress in developing the photomultiplication (PM) phenomenon based high gain inorganic-organic hybrid broadband photodetectors using polymer/inorganic nanocomposites has been observed [11], [12]. For the first time, Rouch et al. [29] have reported a PbS: P3HT(Poly(3-hexylthiophene-2,5-diyl): PCBM ternary blend photodetector with responsivity and normalized detectivity of 0.5 A/W and 2.3x109 Jones respectively. R. Dong et al.[28] reported a P3HT: PCBM: PbS: ZnO QDs organic-organic quaternary nanocomposite based broadband photodetector with responsivities of 4.58 A/W at 350 nm (UV), 5.60 A/W at 500 nm (Visible), and 1.23 A/W at 930 nm (NIR); and the maximum external quantum efficiency (EQE) of ~1624 % (350 nm) ,1391%(500 nm) and

166 % (930 nm) at - 4V bias. This high EQE was attributed to the electron trapping at ZnO QDs which enabled photocurrent multiplication (PM) phenomenon inside the device. They used the PbS QDs as NIR sensitizer to extend the detection range to NIR region [28]. F. Guo et al.[27] observed the photomultiplication effect in a ZnO NPs /PVK based ultra-high gain photodetector due to the interfacial charge trap triggered charge injection from the external circuit. Li Shen et al. [77] reported that NPs-rich surface near the cathode electrode may influence the photoconductive gain of the photodetectors by charge tunnelling injection phenomenon.

In general, PEDOT: PSS is widely used for the HTL in most of the conventional structure based organic photodetectors[81]. However, it is reported that PEDOT: PSS based HTL may contaminate the active polymer layer which, in turn, may affect the performance of the device [82]. That is why, an inverted structure is usually preferred to avoid any such contamination from the PEDOT: PSS based HTL. Further, usually a a nanostructured material-based electron transport layer (ETL) is usually preferred over the bulk material based ETL in a photodetector to improve the carrier transportation and collection due to its inherently higher surface to volume ratio over the bulk. Martinson et al.[83] have observed improved carrier transport, reduced recombination and enhanced collection of photogenerated carries in dye-sensitized solar cells by using a ZnO NRs-based ETL structure. Significant improvements in the solar cell performance was observed by allowing ZnO NRs to penetrate into the active layer. Photo-generated electrons travel a very short distance to reach any of the NRs of the ETL penetrated into the active layer, faster collection of the photo-generated carriers with a significantly reduced recombination rate is possible in such photodetectors [84]–[86].

In view of the above discussion, the present chapter is devoted to investigate the performance characteristics of an FTO/ZnO NRs/PCDTBT: PCBM: PbS QDs/MoOx/Ag organic-inorganic nanocomposite-based inverted structure hybrid broadband photodetector. The ZnO NRs layer acts for both the ETL as well as a surface with intrinsic traps near the cathode electrode which can enhance the photocurrent due to the photomultiplication effect resulted from the induced charge tunnelling from the external circuits[56], [57], [73]. The ZnO NRs are allowed to be penetrated into the active layer to reduce the dark current due to recombination as discussed earlier. The PCDTBT: PCBM composite is chosen due to its ultra- fast exciton dissociation phenomenon [26] and PbS QDs in the PCDTBT:PCBM:PbS QDs nanocomposite are used to extend the spectral range of the nanocomposite in the NIR region. The ZnO NRs also act the electron transport layer (ETL) and the conventional PEDOT: PSS is replaced by MoOx HTL to avoid any sort of contamination.

2.2 Experimental Methodology

In this section, materials used and their synthesis methodology such as synthesis procedure has been discussed in detail.

2.2.1. Materials Used and Synthesis

All chemicals are procured and used as it is without any further purification from Sigma-Aldrich and Merck Chemicals.For synthesis of the ZnO nanorods, fluorine-doped tin oxide (FTO) coated glass substrates are used after ultrasonically cleaning for 5 min each in a soap solution, deionized water (DI water) and acetone respectively. A seed layer of ZnO quantum dots (QDs) were spin cast on the FTO substrate. ZnO QDs were synthesized by following our previously reported work [87]. In this method, Zinc acetate dihydrate (0.5M) was mixed with

2-methoxy ethanol. The solution is stirred for 1 hour under a gradual increase of temperature up to 60oC. At this temperature, monoethanolamine (MEA) was quickly injected into the solution. The solution was then kept for 24 hours under continuous stirring in a nitrogen environment. Finally, the solution was deposited on FTO substrate by spin coating method to form a ZnO QDs based thick seed layer of ~50 nm. ZnO nanorods arrays (NRAs) are then grown on the seed layer coated fluorine-doped tin oxide (FTO) substrates by simple cost-effective hydrothermal process[32].

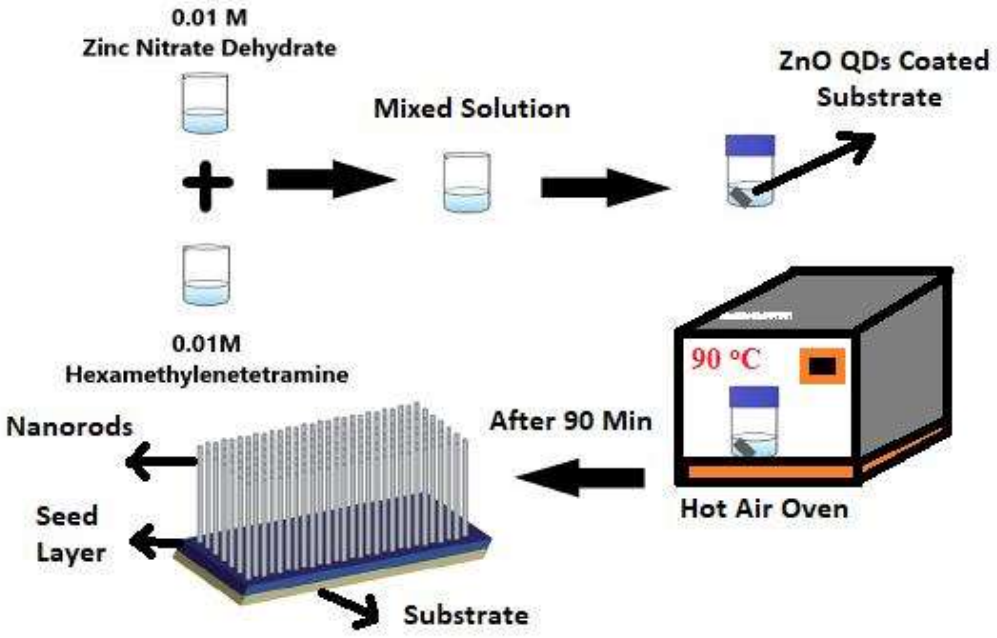

Fig. 2.1 Represents the schematic of Hydrothermal synthesis of ZnO nanorods FTO glass substrate

The seed layer coated samples were dipped in an equimolar solution of zinc nitrate dehydrate (0.01M) and hexamethylenetetramine (0.01M) maintained at 90 ^{o}C for 90 minutes to grow ZnO NRAs. Samples were then washed vigorously with deionized (DI) water and were

annealed at 400°C for 30 min in air environment before use. The procedure of hydrothermal synthesis of ZnO NRs preparation is pictorially shown in Fig.2.1

2.2.2. Device Fabrication

The annealed ZnO NRAs coated FTO substrates were plasma etched in the argon environment for 5 min [88]. For preparing the material used in the active layer, PCDTBT and PCBM were separately dissolved in 1, 2 Dichlorobenzene and chloroform respectively for 15 hours under continuous stirring. Then, the PbS QDs solution procured from Sigma Aldrich of concentration 10 mg mL-1 were mixed in PCDTBT solutions and kept under stirring for two more hours. Finally, solutions of PCDTBT: PbS QDS and PCBM were mixed and then again kept for 2 hours under continuous stirring. The PbS QDs solution of concentration 10 mg mL^{-1} was added to the PCDTBT maintaining PCDTBT, PCBM and PbS QDs ratio of 1:4:0.5 by weight with respective concentrations of 5, 20, and 2.5 mg mL^{-1} respectively. The PbS QDs solution was used as procured without any ligands exchange. The ternary blend composite is then deposited on the ZnO NRAs and ZnO QDs thin film by spin coating method. The organic active layer was then annealed in air for 10 min at 120°C. Thermal evaporation was used to deposit a thin layer (~ 12 nm) of MoOx on the active layer at vacuum level of ~ 3x10-6 mbar. Finally, silver (Ag) thin film of ~120 nm thickness was deposited in the form of circular dots on the top of MoOx layer using mask of 2 mm diameter[89]. Thus, effective area of the active layer under each of Ag circular contacts is 0.0314 cm^2.

2.3 Results and Discussion

In this section, material ,electrical and as well as optical characterization of the fabricated device are presented in details.

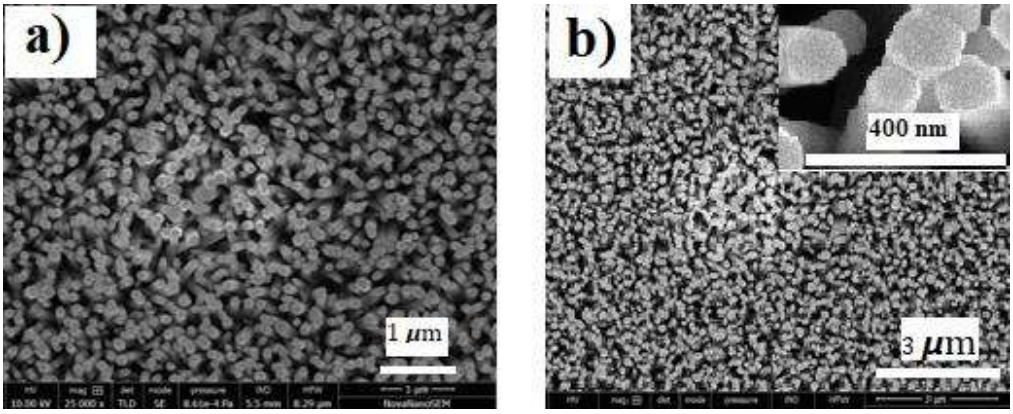

Fig. 2.2 High-resolution SEM image of ZnO NRAs on FTO glass substrate (a) 1 μm Scale (b) 3 μm Scale. Top right inset in (b) is the corresponding enlargement.

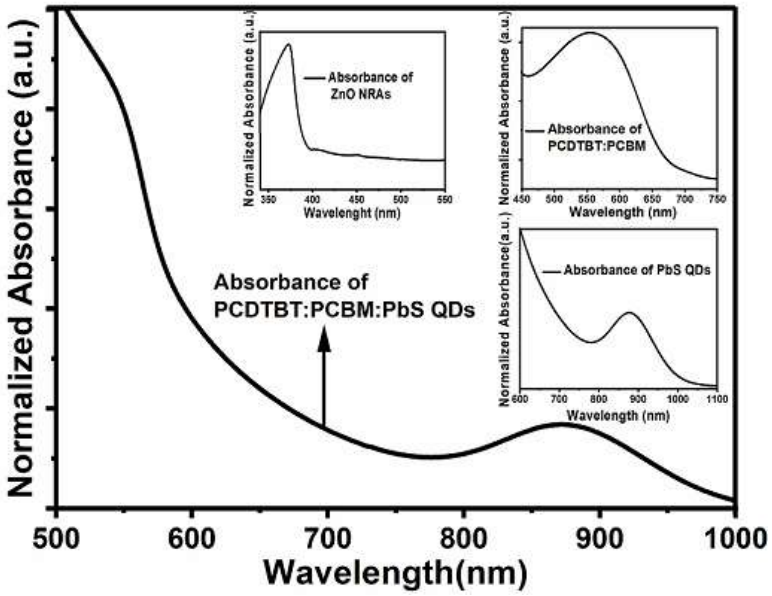

Fig.2.3 Shows the absorbance plot of PCDTBT: PCBM: PbS QDs Ternary blends Nano Composite active layer. Inset shows the separate absorbance spectrum of ZnO NRAs, PbS QDs and PCDTBT: PCBM Composite.

2.3.1 Material and Electrical Characterization

Fig.2.2 (a), (b) shows the high-resolution SEM (HRSEM) image of the ZnO NRAs grown on the FTO coated glass substrate. The as-grown well-aligned vertically ZnO NRAs have a

hexagonal cross-section evident from HRSEM image (Inset). The absorption spectra of PCDTBT: PCBM: PbS QDs nano-composite is shown in the Fig.2.3. The separate absorption spectra of ZnO NRAs, PCDTBT: PCBM and PbS QDs give the individual absorption peak at ~380 nm (UV),~550 nm (Visible) and ~860 nm (NIR) regions respectively (shown in inset). The PbS QDs in the active layer thus not only acts as a sensitizer but also acts to broaden the absorption spectrum of the PCDTBT: PCBM: PbS QDs active layer from visible to NIR by adding an additional peak at ~ 860 nm (NIR).

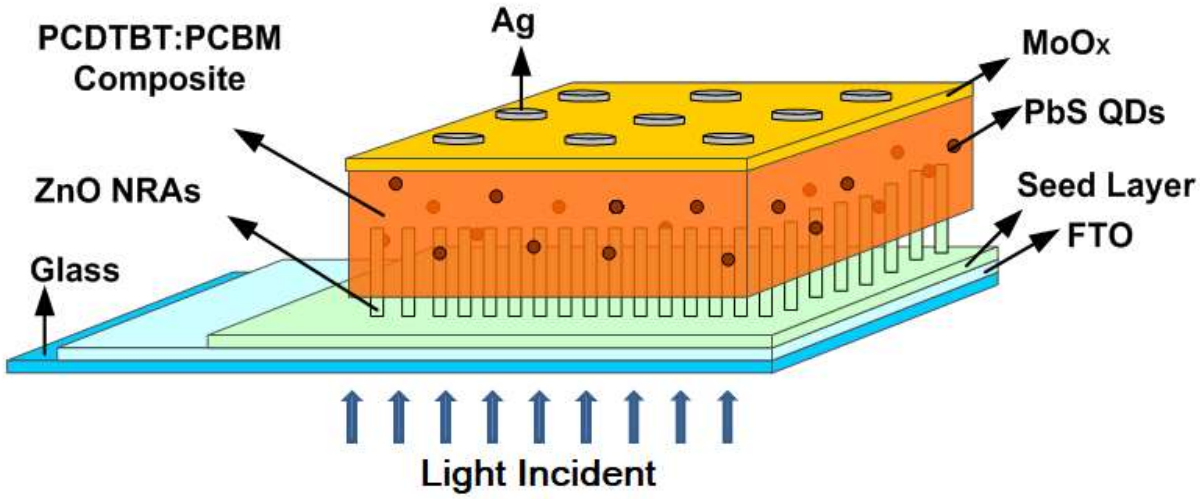

Fig. 2.4 : Schematic representation of inverted broadband photodetector Device structure (Light illumination from glass Side)

The proposed device structure and the charge transfer mechanism in the proposed structure are shown and illustrated in Fig.2.4 and Fig.2.5 respectively. As evident from the energy band diagram that the holes are transferred from PbS QDs to PCDTBT and electrons are transferred from PbS QDs to PCBM respectively. The photo-generated electrons and holes under illumination are finally transported through the ZnO NRAs and MoOx layers to result in the

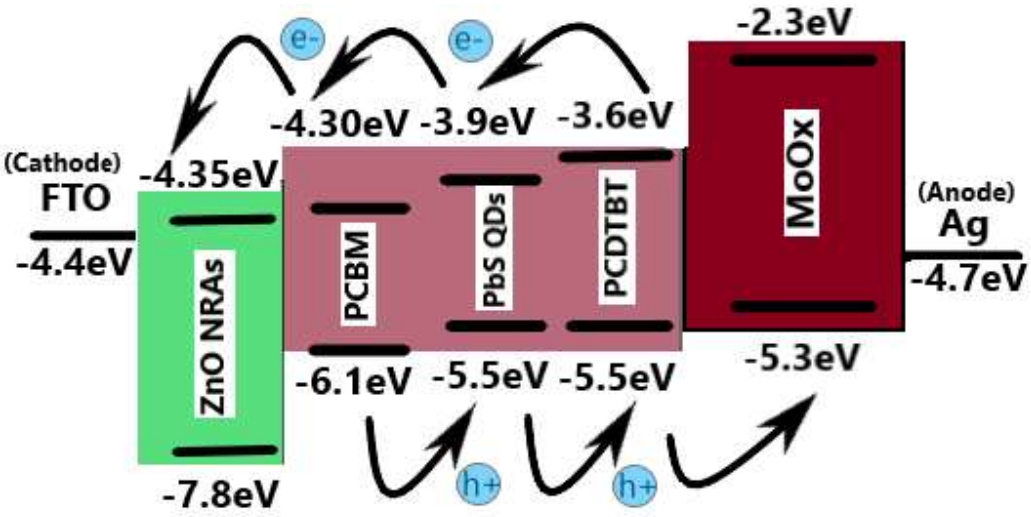

Fig. 2.5: Energy band diagram under Light Illumination at -1.5V bias.

photocurrent of the device [90]. The step-like band alignment ensures effective charge transfer in the proposed photodetector. X.Wang et al.[91] and Y.Wei et al. [92] have successfully demonstrated that proper energy band alignment leads to the high performance of the photodetectors device. Large ΔEc leads to more energy loss which results in poor responsivity [93]. In our device we have incorporated PbS QDs into active layer not only to broaden absorption spectrum of PCDTBT: PCBM and as a sensitizer but also to reduce some energy loss which results due to large ΔEc (the difference between the conduction band of PCDTBT and PCBM). Incorporation of PbS QDs may circumvent these problems by reducing ΔEc as evident from the schematic energy band diagram shown in Fig. 2.5.

The electrical characterization of the device was performed under an ambient air environment using a parameter analyzer (Key sight: Model B1500A).Fig.2.6 shows the semi-logarithmic J-V Plot of ZnO Nanorods penetrating ETL and non-penetrating ZnO thin film ETL based device. The non- penetrating thin film-based device shows typical photovoltaic behaviour under light.

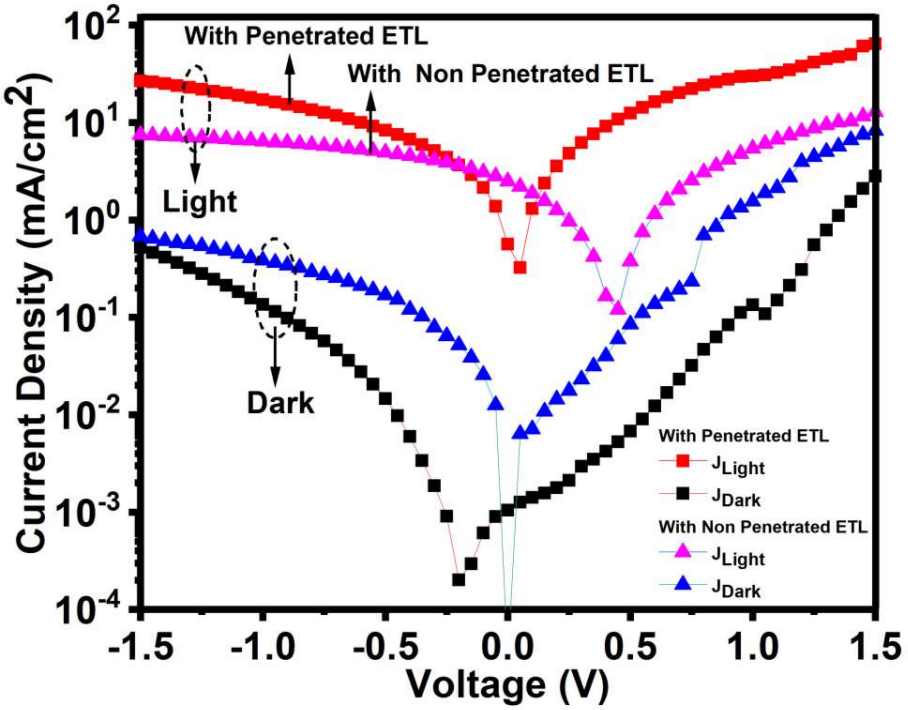

Fig. 2.6: Semi logarithmic J-V Plot of ZnO nanorods based Penetrated ETL device and ZnO thin film based non penetrated ETL device at dark and under illumination light of intensity 100 mW/cm^2.

These photovoltaic effects disappear completely with the introduction of penetrated ZnO NRAs ETL into active polymer –fullerene composites, as introduced ZnO NRAs act as a charge trap. It is eminent from J-V Plot that the photocurrent of ZnO NRAs based device is greater than the non-penetrating thin-film ETL based device this gives clear evidence of photo induced charge injection [28].

2.3.2 Optical Characterization

The optical measurement is carried out by using monochromator (SP2150i from Princeton Instruments, USA). The responsivity and EQE is determined from the following equations [32].

$$R_\lambda(A/W) = \frac{I_{ph}}{P_{in}}, \quad (2.1)$$

$$EQE(\%) = 1240\frac{R_\lambda}{\lambda} * 100 \quad (2.2)$$

Where, R_λ is the responsivity in (A/W) and λ is wavelength in (nm), I_{Ph} is the measured photocurrent and P_{IN} is the incident optical power on the device.

The Detectivity (D) is also calculated by using the following equation mentioned below[31].

$$D(Jones) = \frac{R_\lambda}{\sqrt{2eJ_d}} \quad (2.3)$$

Where J_d is the dark current density (A/cm2) and e (C) is the electron charge

Calculated values of responsivity under – 1.5 V external bias at three selected wavelengths in UV (380 nm), Visible (550nm) and NIR (860 nm) regions are ~213.77 A/W, ~28.57 A/W and ~7.22 A/W respectively.

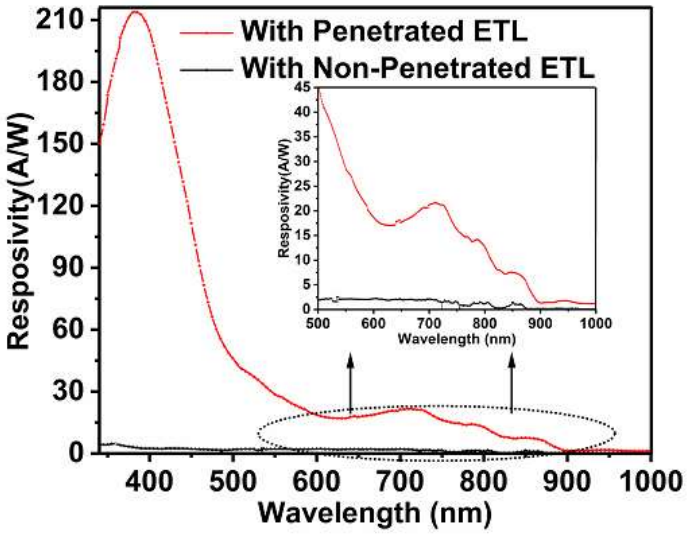

Fig. 2.7: Responsivity plot showing comparison of ZnO nanorods penetrated and ZnO thin film non penetrated ETL based device. Inset shows the significant enhancement in visible and NIR region.

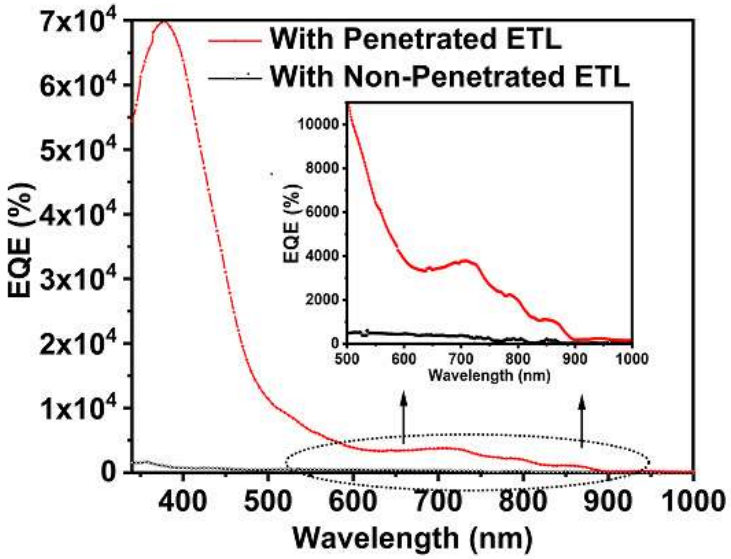

Fig. 2.8 : Shows the EQE plot depicting the comparison of ZnO nanorods penetrated and ZnO thin film non penetrated ETL based device. Inset shows the significant enhancement in visible and NIR region.

The corresponding responsivity curve as a function of wavelength with both penetrated ZnO layer as well as non-penetrated layer is shown in the Fig.2.7.The high EQE values are also measured at the same operating bias with ~ 69779 % (UV-Region),~ 6464 % (Visible Region) and ~1047% (NIR Region) respectively.

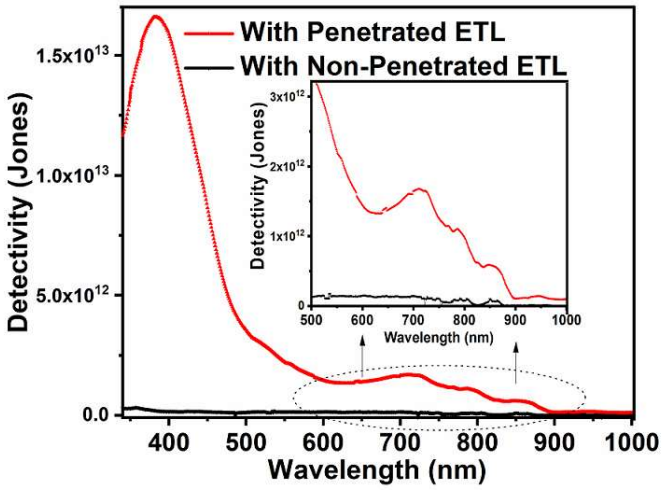

Fig 2.9: Detectivity plot as a function of wavelength under -1.5 V bias showing device detectivity comparison with and without penetrated ETL.

The corresponding EQE curve as a function of wavelength with both penetrated ZnO layer as well as non-penetrated layer is depicted from the Fig.2.8.Similarly, detectivity are also calculated by using equation 2.3 under -1.5 V bias. The corresponding detectivity values at 380 nm ,550 nm and 860 nm are 1.65x1013 Jones,2.21x1012 Jones and 5.82x1011 Jones respectively. The curve of Detectivity as a function of wavelength is shown in the Fig 2.9. Noteworthy values of EQE above 1000% and high values of responsivity as well as detectivity was observed in our proposed photodetector over a broad spectral range. Notable performance in our device is attributed to number of electrons that are trapped in the ZnO NRAs of the ETL. These trapped electrons reduce the barrier for hole injection by bending the energy band near the cathode under the reverse bias operation of the device. This favors photomultiplication in the device under reverse bias to cause the EQE above 100% [28].

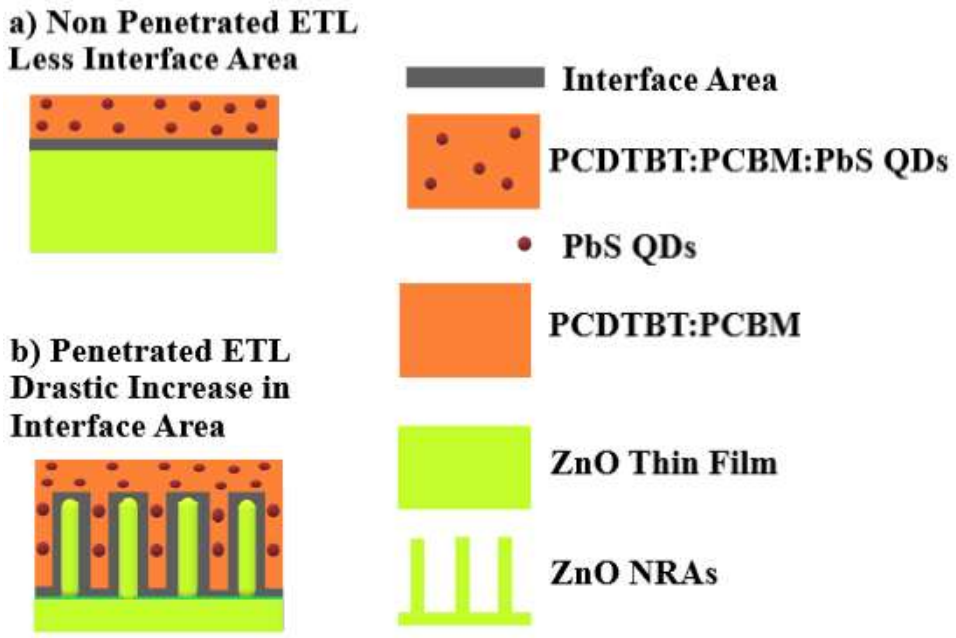

Fig. 2.10: Pictorial illustration of Interface Area (Light interaction Volume) with (a) planar and (b) penetrated device structure

From the Fig. 2.7, Fig 2.8 and Fig 2.9, we can see that the proposed device shows drastic performance enhancement in responsivity, EQE and detectivity over a broad spectral range from UV to NIR. The enhancement of the UV responsivity is attributed to large interface area and higher light interaction volume in penetrated ETL based device. Fig.2.10 illustrates pictorially how the ZnO NRAs (penetrated ETL)/Active Layer based device exhibits larger interface area which in turns leads to higher light interaction volume as well as generates more number carriers.

The responsivity of photodetector is considered as one of the important parameters basically used to explain the photoelectric conversion capability of the fabricated device. Measurement shows that improvement of responsivity is observed over broad spectral range from UV to NIR for penetrated ZnO NRAs electron transport layer-based device.

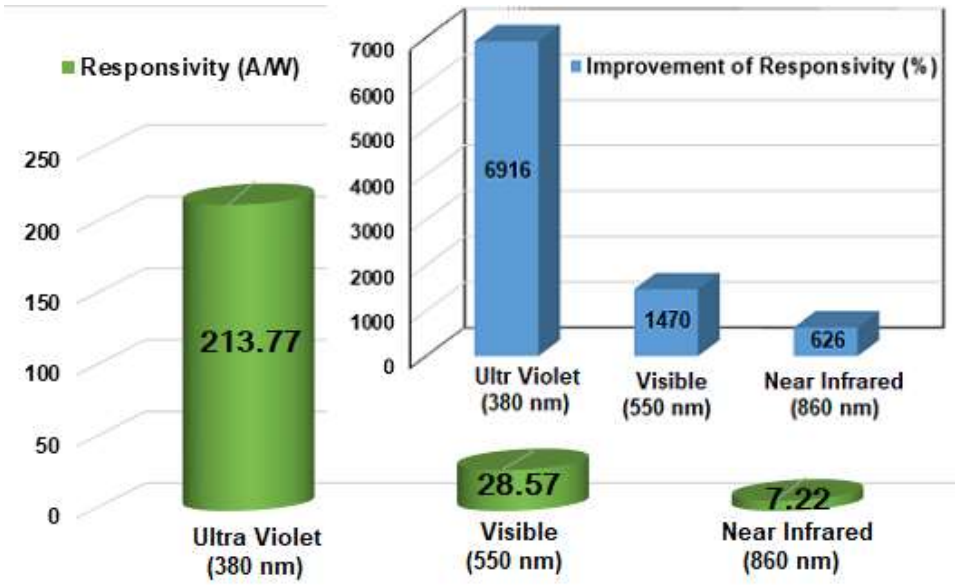

Fig. 2.11 : Graphical illustration of improvement of the responsivity at three selected wavelengths by introducing penetrated ZnO NRAs ETL in PCDTBT: PCBM: PbS QDs composite System.

The penetrated ETL based device not only shows the drastic enhancement on UV responsivity but significantly good improvement in Visible as well as NIR responsivity is also observed as compared to non-penetrated ETL based device. Interestingly, with ZnO NRAs (Penetrated ETL) device the performance is significantly enhanced in visible as well as NIR bands. The drastic improvement in the fabricated device responsivity (%) parameter as a function of wavelength under -1.5 V external bias is visualize from the graphical representation as shown in Fig.2.11.

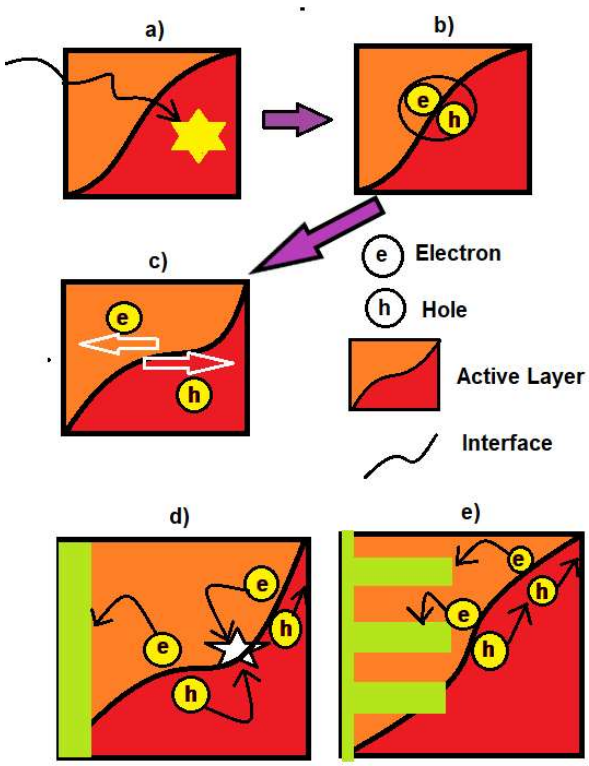

Fig.2.12: Mechanism of photocurrent generation, photocurrent losses and strategy to reduce such losses. (a) Generation of exciton by absorption of photon in the active layer. (b) After photon absorption charge transfer state is created at the interface. (c) separation of charge carrier as free charge carrier followed by charge transport through the bulk materials of the active layer. (d) Device with non-penetrated ETL results in somewhat more recombination of free charge carrier with in the active layer itself before reaching to electrodes. (e) Device with penetrated ETL reduces the probability of free charge carrier recombination.

The mechanism behind the enhancement in Visible and NIR bands are elucidated from the physics of PCDTBT: PCBM which reveals that the presence of large energetic disorder in the PCDTBT introduces a large number of low energies polarons with limited mobility. These polarons enhance the recombination rate in the conventional PCDTBT:PCBM based active layer [85].Thus, an improved charge extraction strategy is required to enhance the performance of such photodetectors by minimizing the effect of the high recombination rate. The ZnO NRAs based ETL results in the penetration of the NRAs inside the polymer active layer to enhance the extraction and collection of photogenerated carriers in the active layer by reducing the probability of recombination [94].

Pictorial illustration of improved charge extraction strategy is shown in Fig.2.12. As most of the organic materials exhibits short exciton lifetime which in turn leads to small exciton diffusion length of about only 10 nm [95]–[97].This shot exciton lifetime limits the performance of the device. Hence, efficient harvesting of exciton is only possible if the exciton has to diffuse very small distance. The exciton harvesting is one of the important factors responsible for polymer broadband photodetector performance. So penetrated ETL into the active layer results in better charge extraction and collection strategy as compared to thin film non penetrated ETL . We have compared the responsivity , EQE and detectivity curve of our proposed device as a function of wavelength at -1.5V external bias with that of the device using a simple ZnO thin film based ETL as shown in Fig.2.7 , 2.8 and Fig.2.9 over broad spectral range from UV to NIR.

The penetration of NRAs into the active layer enhances both the responsivity and EQE due to surface trap induced carrier injection into the ZnO NRAs ETL [10], [16] as well as greater light interaction volume (larger interface area). Thus, the extremely high responsivity and

EQE of our proposed PCDTBT: PCBM: PbS QDs based photodetector may be attributed to the simultaneous effects of efficient charge collection strategy through penetrated ZnO NRAs (ETL) and ultrafast exciton dissociation phenomenon in PCDTBT: PCBM[26], [31].Table-I shows a comparison of our results with some other organic materials based polymer broadband photodetectors reported in the literature. Note that our proposed device shows extremely high-performance organic photodetectors.

TABLE. I Comparison of some Organic Materials based Photodetectors

Materials Used	**Inverted Structure (Bias)**	**ETL**	**Spectral Range (nm)**	**R (A/W)**	**EQE (%)**	**Ref.**
TiO_2 NCs/P3HT:PCBM	YES (-1 V)	Non-Penetrated TiO_2 NCs	350-650	0.2 @ 370 nm 0.5 @ 550 nm	113 @ 550 nm	[98]
ZnO/P3HT:ITIC	YES (-20 V)	Non-Penetrated ZnO	300-800	-------	19300 @ 360 nm	[99]
PEDOT:PSS/P3HT:PTB7-Th:PCBM	NO (-25 V)	NO	300-800	284.9@ 390 nm 423.4 @ 625 nm 5.2 @ 750 nm	90700 @ 390 nm 84100 @ 625 nm 850 @ 750 nm	[100]
ZnONW/PDDTT:PCBM	YES (0 V)	Penetrated ZnO NW	400-1450	0.18 @ 800 nm	27 @ 800 nm	[31]
ZnO/PCPDTBT:PCBM	YES (0.5)	Non-Penetrated ZnO	400-850	---------	< 40 range 400-850	[101]

Materials Used	**Inverted Structure (Bias)**	**ETL**	**Spectral Range (nm)**	**R (A/W)**	**EQE (%)**	**Ref.**
PEDOT:PSS/P3HT:PCBM:PbS QDs: ZnO QDs	NO (-4 V)	NO	300-1100	4.58 @ 350 nm 5.60 @ 500 nm 1.24 @ 930 nm	1624 @ 350 nm 1391 @ 500 nm 166 @ 930 nm	[28]
PEDOTPSS/F8T2:ZnO NPs	NO (-15 V)	NO	300-600	6.39 @ 360 nm 0.89 @ 510 nm	2170 @ 360 nm 220 @ 510 nm	[21]
ZnO NRAs/ PCDTBT: PCBM: PbS QDs	YES (-1.5 V)	Penetrated ZnO NRAs	350-1000	213.7 @ 380 nm 28.57 @ 550 nm 7.22 @ 860 nm	69779 @ 380 nm 6464 @ 550 nm 1047 @ 860 nm	**This Work**

2.4 Conclusions

In this chapter, the goal is to develop a novel strategy for enhancing the responsivity, Detectivity and external quantum efficiency (EQE) of a PCDTBT: PCBM: PbS QDs ternary blend nanocomposite-based hybrid broadband photodetector by ETL engineering as well as active layer engineering. The main idea of present chapter is to induce band bending near the cathode electrode charge tunnelling injection from the external circuits to attain photoconductive gain. In this chapter the effect of penetrated ZnO NRs is investigated with

ternary blend active layers. The proposed device in the chapter utilizes ZnO nanorods as a penetrated ETL layer, while PCDTBT: PCBM composite is considered in the present study due to its ultra- fast exciton dissociation phenomenon [26]and MoOx is used as a hole transport layer. The PbS QDs are used for enhancing the absorption in the near infrared region of the active layer. The active layer comprises of PCDTBT:PCBM:PbS QDs is deposited by spin coating technique on the vertically grown penetrated ZnO nanorods. The fabricated device optical characterization of the give's high values of responsivities, EQEs and detectivities of about ~213.77 A/W, ~69779% and $1.65x10^{13}$ at 380 nm (i.e., in the UV region); ~28.57 A/W, ~6464% and $2.21x10^{12}$ at 550 nm (i.e., in the visible region); and ~7.22 A/W, 1047% and $5.82x10^{11}$ at 860 nm (i.e., in the near NIR region) measured under -1.5 V